This article has been accepted for publication in IEEE Transactions on Power Systems. This is the author's version which has not been fully edited and content may change prior to final publication. Citation information: DOI 10.1109/TPWRS.2023.3279364

Enhanced DC Voltage and Frequency Regulation for High Voltage AC/DC Power Grid

Biyadgie E. Ayalew, Mohamed Shawky El Moursi, *Senior member, IEEE,* and Ehab F. El-Saadany, *Fellow, IEEE*

***Abstract*—This work proposes a primary frequency support mechanism for a voltage source converter (VSC) based multi-terminal high voltage dc (MTDC) transmission system that interconnects asynchronous ac grids. For the ac disturbance case, an augmented control strategy composed of a coordinated droop control (CDC) and a supplementary controller is developed. In CDC, the droop constants are determined considering the desired disturbance sharing ratio among the ac areas and the loading of the converters. On the other hand, the supplementary controller makes the designed droop constants provide the expected performance independent of the dc network parameters and the VSCs power losses. Therefore, the augmented controller can make the interconnected ac power systems exchange power according to the specified disturbance sharing ratio. In addition, the work introduces a new power rerouting technique to enhance the frequency and the dc voltage regulation of the ac/dc power system when a VSC trips. Furthermore, the droop constants for the nominal operation are designed to make the ac grids share the disturbance due to wind farm power variation based on their strength. Case studies are conducted for evaluation, and the presented technique shows enhanced performance in frequency (for instance, 38% improvement when ac disturbance happens) and dc voltage (for example, almost zero deviation when converter outage occurs) regulations compared to the existing mechanisms in the literature.**

***Index Terms*—Supplementary controller, novel power rerouting mechanism, impact of dc grid and VSCs power losses, coordinated droop gain scheme, frequency support, enhanced dc voltage response, converter outage, MTDC system.**

I. Introduction

In the last decades, lots of research work have been carried out to develop frequency support strategies for voltage source converter (VSC) based multi-terminal HVDC (MTDC) transmission system. MTDC system has the potential to be the best solution for the integration of renewable energy power systems to the main ac grids because of its high flexibility and reliability features compared to the two terminal HVDC link. However, because of the decoupling nature of the HVDC system, the interconnected ac grids can't share their spinning reserve during contingencies unless there is a mechanism deployed in the controller of the MTDC system. Also, the intermittent behavior of the renewable energy resources can make the frequency of the ac grids vulnerable. Therefore, different strategies have been proposed to enable ac grids share their reserve in response to frequency disturbance in any one of them.

Some works focus on the secondary frequency control to restore the frequency to the nominal value [1]–[3]. On the other hand, extensive research works have been done to develop primary frequency support schemes for MTDC system. Generally, the mechanisms can be categorized as communication-free and communication-based. The communication-free control strategies depends on $P - V_{dc} - f$ droop control are reported in [4], [5]. Although being communication-less has cost wise advantage, the extent that ac areas can support each other isn't clearly defined. Also, the mechanisms have significant steady-state dc voltage deviation due to lack of coordination among converters. Reference [6] augments a mechanism to the conventional virtual synchronous generator (VSG) controller to upgrade the performance of VSG in frequency support. However, the extent of support among ac grids isn't well defined similar to [4], [5]. Also, the performance of the technique is affected by the dc grid parameters and the power losses of VSCs since the augmented controller is based on $P - V_{dc}$ droop control. In [7], [8], a variable droop gain scheme based on the conventional $P - V_{dc} - f$ was proposed to make the supporting ac grids inject more power to the dc grid. The droop gains are made vary according to the frequency deviation of the ac grids. A similar mechanism like [7] but with different strategies to keep the dc voltage within the permissible range during frequency support is reported in [9], [10]. On the other hand, in [11], integration based frequency support was proposed to restore the frequency to the nominal value. However, in schemes [7]–[11], there isn't coordination among the supporting ac grids. Therefore, there can be a disproportionate burden allocation to the supporting ac grids in the time of frequency support.

Various communication-based frequency support mechanisms are reported in the literature. Reference [12] discussed a centralized optimization based strategy, that needs fast speed signal transmission system to and from the central control station, to determine the proper spinning reserve exchange among the ac grids. However, the reported scheme has drawback of high computational burden needed to solve the objective function online. Also, the constraints of the cost function focus only on limiting the rate of change of the frequency (RoCoF) during disturbances. There aren't discussions on primary frequency support. In addition, the presented optimization function didn't consider the dc voltage deviation. A different control strategy is presented in [13] in which the converters in the affected ac power system operate as ac slack bus mode. As ac slack bus, the converters try to maintain the frequency of their ac grid by exporting power from the dc system. On the other hand, the power unbalance created on the dc system

This work was supported in part by Khalifa University under Award No. [CIRA-2018-37] and in part by ASPIRE, Technology Program Management Pillar of Abu Dhabi's Advanced Technology Research Council (ATRC), through ASPIRE Virtual Research Institute (VRI) Award.

Biyadgie Ayalew, Mohamed Shawky El Moursi and Ehab F. El-Saadany are with the Advanced Power, and Energy Center, EECS Department, Khalifa University, Abu Dhabi 127788, UAE (emails: biyadgie.ayalew@ku.ac.ae , mohamed.elmoursi@ku.ac.ae , ehab.elsadaany@ku.ac.ae). Mohamed Shawky El Moursi is also with the Faculty of Engineering, Mansoura University, Mansoura 35516, Egypt.

This article has been accepted for publication in IEEE Transactions on Power Systems. This is the author's version which has not been fully edited and content may change prior to final publication. Citation information: DOI 10.1109/TPWRS.2023.3279364

will be covered by the converters in the undisturbed ac power systems. However, in this mechanism the entire disturbance is carried by the healthy ac grids. Therefore, their frequency can deviate significantly. Moreover, the communication network, used by the control systems of the undisturbed converters to determine the amount of power to be injected to the dc grid, is required to have high bandwidth.

Another communication based technique is reported in [14] to avoid the dc voltage deviation during frequency support. However, similar to [4] and [5], there isn't clear definition on how the burden due to a contingency is allocated to the participant ac power systems. Reference [15] presents an extension of the work in [14]. In [15], converters activate the full support to their interfaced ac grid when the frequency deviation passes the specified threshold level. For this, the droop gains are designed considering the planned maximum power support and the threshold frequency deviation. Moreover, the reported work tried to make sure that the droop gains perform as per their design. However, the coordination among the ac grids to manage the burden during frequency support according to their size is still missed. In [16]–[18], average consensus algorithm is employed for the primary frequency support, and the weights in the algorithm are used to define the proportion that the ac areas share the disturbance. In other studies presented in [19], a mechanism is developed to make frequency support only from the strong to the weak ac grids. However, the strategies in [15]–[19] rely on high bandwidth signal transmission system used to transmit the data of the frequency deviations as input to the control system.

Methods with less communication dependency are presented in [20]–[23]. The reported schemes depend on the conventional frequency droop ($P - V_{dc} - f$) control; however, similar to the consensus algorithm, weighted based strategy is used to distribute the burden among the participant ac grids. In [20]–[22], the distribution of duty among the converters doesn't consider their actual available headroom. The converters are given responsibility based on their rating capacity. Therefore, the required power may not be traded among the interconnected asynchronous ac areas during frequency support if there are converters that are already fully occupied. As a solution, [23] proposed frequency support strategy that takes the loading of the converters into account. However, the reported scheme can be affected by the dc network parameters and the VSCs power losses as they are neglected in the formulation of the technique. Moreover, the frequency disturbance on the ac grids due to wind farm power variation isn't addressed.

The above discussions present the comparison of the existing mechanisms based on their performance in minimizing the frequency deviation during an ac disturbance. However, converter outage also impacts the frequency of the ac power systems. References [4], [16], [21] employs the same method used for ac disturbance to lessen the consequence of converter tripping on the frequency of ac grids. However, in the time of converter tripping, the frequency deviation is because of the perturbations in the power transmission between the dc and ac systems, unlike ac disturbance which causes the frequency deviation due to ac load increment or decrements in ac grids. Therefore, different approaches are proposed in [12], [22]–[24] to obtain a more enhanced frequency response. References [24] used an online optimization technique to re-establish the power flow between the dc and ac systems by redistributing the tripped converter power before the disturbance to the survivor converters according to their loading condition. However, finding the optimal solution online isn't feasible for a complex power system. In [22], an offline optimization method is proposed to determine the required power and dc voltage reference changes that can reduce the frequency deviation. The reported technique depends on the scheduled power and dc voltage settings to calculate the required changes of the references. However, the loading of converters can vary from their schedule settings due to wind farm power variation or ac disturbance. Therefore, the pre-determined reference changes may not achieve the desired performance when converter outage occurs. Reference [12] presents an optimization technique by considering the estimation of day-ahead wind energy production and load variation to limit the ac grids' rate of change of frequency (RoCoF) due to converter outage. However, the mechanism didn't consider the steady-state frequency deviation. Recently, [23] proposed a methodology that tries to eliminate the aftermath of converter tripping on the frequency of the interconnected ac power systems. However, in the presented technique, the dc voltage deviation is significant.

In this research, we propose a frequency support technique for the MTDC system to enhance the regulation of the dc voltage and ac frequencies of the hybrid ac/dc grid during contingencies. The mechanism consists of the combination of the proposed supplementary controller and coordinated droop gain scheme for ac disturbance, novel power rerouting management during converter outage, and a strategy to minimize the stress on the ac grids frequency when there is wind farm power variation. Moreover, the presented mechanism uses a low bandwidth communication network for coordination and relevant information exchange among converters. The major contributions of the proposed mechanism can be summed up as follows.

- Developing an augmented controller consists of coordinated droop control (CDC) and supplementary controllers. Therefore, the droop gains of the CDC will perform as per design to achieve the specified percentage of power sharing among the interconnected ac grids during ac disturbance by overcoming the impact of the dc grid parameters and VSCs power losses.
- Developing a new power rerouting scheme to enhance the dc voltage and frequency regulation in the ac/dc power system during converter tripping.
- Introducing a dc voltage droop gains design methodology considering the stress on ac power systems frequency due to wind farm power variation.
- Establishing a coordination strategy to activate the proper frequency support technique according to the type of disturbance.

The organization of the rest of the manuscript is described in the following. In section II, the basics of disturbances that cause frequency and dc voltage deviation, and selected frequency support techniques are discussed. On the other hand, the overall operation of the proposed scheme is presented in section III. Section IV and V talk about the proposed supplementary controller and the nominal droop gain design procedures accordingly. The proposed strategy for scenario of converter tripping is discussed in section VI. The simulation results and their detailed discussions are available in section VII. Finally, section VIII presents the conclusion.

II. Causes of power unbalance in the ac/dc grid and Selected frequency support schemes

This section highlights the causes of power deviation in ac grids interconnected by MTDC system. Also, the brief discussion of selected frequency support schemes is presented.

A. Causes of power unbalance in the ac/dc grid

Power unbalance in the ac/dc grid can happen due to ac disturbance, converter outage and the change in windfarm power production. In the following, the nature of the power unbalance during each disturbance will be discussed. The explanation will be based on the consideration that the MTDC system doesn't have frequency support scheme. Later, selected frequency support techniques will be described.

1) Power unbalance due to ac disturbance: When an ac grid faces load change, the other ac grids won't sense the disturbance due to the decoupling by the MTDC system. Therefore, only the frequency of the disturbed ac grid deviates. Also, there won't be any impact on the dc voltage of the dc grid and frequency of other ac grids. Furthermore, the total power unbalance of the ac/dc system will be the same as the power deviation of that ac grid assuming there aren't any other disturbances in the ac/dc system.

2) Power unbalance due to converter outage: During converter outage, the ac grid with the tripped converter will definitely have power unbalance. On the other hand, the other ac grids face power deviation because the droop controlled converters adjust the power injecting to or from their ac grids to regulate the dc voltage. Assuming a lossless MTDC system, the power deviation of each ac grid can be written as shown in (1) for the ac grid interfaced with the tripped converter and (2) for other ac grids. It is considered that the k^{th} converter trips and is located in ac grid a_j. Also, the dc voltage will be impacted based on the pre-disturbance power of the tripped converter and the dc voltage droop gains [25], [26]. For details of the derivation concerning the dc voltage and ac grids power deviation, the reader can refer to [25], [26].

$$\begin{cases} \Delta P_{a_j} & = -P_k + \dfrac{\sum\limits_{j\in\phi^{a_j}} g_{v,j}}{G_{v,agg} - g_{v,k}} P_k \\ & = P_k \dfrac{\left(-G_{v,agg,a_j} - \sum\limits_{a_k\in S^{ac}} G_{v,agg,a_k} + G_{v,agg,a_j} \right)}{G_{v,agg} - g_{v,k}} \\ & = -P_k \dfrac{\sum\limits_{a_k\in S^{ac}} G_{v,agg,a_k}}{G_{v,agg} - g_{v,k}} \end{cases} \tag{1}$$

where, $G_{v,agg} = \sum\limits_{j\in\phi^{all}} g_{v,j}$, $g_{v,j}$ is the dc voltage droop gain of converters, ϕ^{all} is the set of all droop controlled converters, ΔP_{a_j} is the power deviation of the ac grid, $g_{v,k}$ is the droop gain of the tripped converter, $G_{v,agg,a_j} = \sum\limits_{j\in\phi^{a_j}} g_{v,j}$, ϕ^{a_j} set of survivor converters interfaced to a_j, P_k is the loading of the tripped converter prior to the disturbance and S^{ac} is the set of the interconnected ac grids except the one interfaced with the tripped converter.

$$\Delta P_{a_k} = P_k \frac{G_{v,agg,a_k}}{G_{v,agg} - g_{v,k}}, a_k \neq a_j \tag{2}$$

The power deviations shown in (1) and (2) are the perturbations of the power flow between the ac grids and the dc grid for regulation of the dc voltage. On the other hand, the total power deviation of the ac grids will be zero if we sum (1) and the aggregate of (2).

3) Power unbalance due to windfarm power variation: The power balance of the ac grids is affected due to wind farm power variation because of the droop controlled converters similar to the case of converter outage. For lossless MTDC system, the power perturbation of each grid is expressed as shown in (3) [25], [26]. On the other hand, the total power unbalance of the ac grids will be the same as the power change in the windfarm.

$$\Delta P_{a_k} = -\frac{G_{v,agg,a_k}}{G_{v,agg}} \Delta P_{wf} \tag{3}$$

where, ΔP_{wf} is the power change of the windfarm. Moreover, dc voltage deviation occurs according to the magnitude of ΔP_{wf} and the droop gains [25], [26].

From the above discussions, it can be concluded that the nature of power deviation of ac grids is different for each type of disturbance. During ac disturbance and wind farm power variation, the total power change of the ac girds is different from zero. However, in the case of converter outage, the total power change of the ac grids is zero though there is power unbalance in each ac grid interfaced with the droop controlled converters. On the other hand, the power unbalance during ac disturbance is only in the disturbed ac grid;where as, all ac grids interfaced with the droop controlled converters have power deviations during windfarm power change and converter outage. Remember, the discussion of power unbalance is with the consideration of no frequency support is active in the system. Furthermore, the dc voltage is affected during converter outage and windfarm power change, but not in the case of ac disturbance.

B. Frequency support schemes

1) The conventional frequency droop control ($P - V_{dc} - f$): The $P - V_{dc} - f$ droop control is the common example of frequency support technique and it has the form shown in Fig. 1. In $P - V_{dc} - f$, the converters adjust their power injection according to the frequency deviation of their ac grids. The power balance of a converter is expressed as show in (4).

$$P_{ref,j} - P_j + g_{v,j} \left(V_{dc,ref,j} - V_{dc,j} \right) - g_{f,j} (f_{ref,j} - f_j) = 0 \tag{4}$$

where, $P_{ref,j}$ and $V_{dc,ref,j}$ are the scheduled power and dc voltage references accordingly, and P_j and $V_{dc,j}$ are the actual power and dc voltage in their respective order. As seen in (4), the power injection for frequency regulation is affected by the dc voltage droop control. Therefore, this can reduce the support to the ac grid. On the other hand, trying to reduce the dc voltage droop gains for more frequency support can have detrimental effect on the dc voltage. Considering (4) and the total power balance of MTDC system, the dc voltage deviation during frequency support for the case of ac disturbance and converter outage is obtained as shown in (5) [27]–[29]. It can be seen from (5) that the dc voltage deviation depends on all the frequency changes and frequency droop gains. This strong coupling along with small dc voltage droop gains can cause significant dc voltage deviation. For the case of converter outage, it can be worse since the dc voltage is also influenced by the power of the tripped converter before the disturbance. In (5), $evnt = 1$ and $evnt = 0$ mean ac disturbance and converter outage respectively. Moreover, the frequency droop gains aren't designed considering the size of the ac grids and all the droop gains are fixed. Furthermore, the mechanism doesn't consider the type of the disturbance. Therefore, the conventional $P - V_{dc} - f$ can have poor performance in both frequency and dc voltage regulation.

$$\Delta V_{dc} = \begin{cases} \dfrac{\sum\limits_{j\in\phi^{all}} g_{f,j}\Delta f_j}{G_{v,agg}}, evnt = 1 \\ \dfrac{-P_k + \sum\limits_{j\in\phi^{all}} g_{f,j}\Delta f_j}{G_{v,agg} - g_{v,k}}, evnt = 0 \end{cases} \tag{5}$$

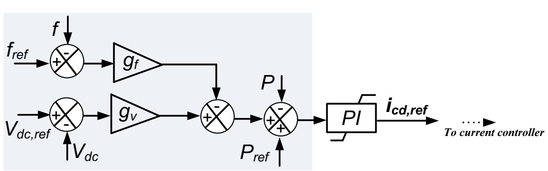

Fig. 1. The structure of $P - V_{dc} - f$

2) Coordinated frequency support scheme (CFSS) [23]: In CFSS, the converters share the burden during frequency support according to their available capacity. Moreover, the strategy for the case of ac disturbance and converter outage is different. As discussed in section II-A, the nature of the impact that ac disturbance and converter outage has on the power balance of the ac grids is different. During ac disturbance, there is a need of net power production or reduction to regulate the frequency. In this regard, the CFSS makes the ac grid to share the burden according to their size and the specified proportions of disturbance sharing. Also, there is a strategy to reduce the coupling between the dc voltage and frequency deviation. For this, the converter interfaced to the affected ac area operates in $P - f$ and those in other (supporting) ac power systems work in $P - V_{dc}$ droop control. Therefore, using the droop relation of the converters depicted in (6) and the MTDC power balance, the dc voltage deviation due to frequency support is obtained as shown in (7). A lossless MTDC system is considered. In (6), $mode = 1$ means $P - V_{dc}$ and $mode = 0$ means $P - f$ droop control.

$$P_{ref,j} - P_j = \begin{cases} -g_{v,j}^{sup}\left(V_{dc,ref,j} - V_{dc,j}\right), mode = 1 \\ g_{f,j}^{dis}\left(f_{ref,j} - f_j\right), mode = 0 \end{cases} \tag{6}$$

where, $g_{v,j}^{sup}$ and $g_{f,j}^{dis}$ are the droop gains of converters in non-affected and perturbed areas respectively. It can be seen from (7) that the coupling is less compared to the $P - V_{dc} - f$ droop control since the dc voltage deviation only depends on the frequency deviation of the affected area (considered to be a_j).

$$\Delta V_{dc} = \frac{G_{f,agg}^{dis}\Delta f_{a_j}}{G_{v,agg}^{sup}} \tag{7}$$

where, $G_{f,agg}^{dis} = \sum\limits_{j\in\phi^{a_j}} g_{f,j}^{dis}$ and $G_{v,agg}^{sup} = \sum\limits_{j\in\phi^{sup}} g_{v,j}^{sup}$, ϕ^{a_j} and ϕ^{sup} are set of converters in the affected and supporting ac grids accordingly. The droop gains for $P - V_{dc}$ and $P - f$ droop controls are determined considering the swing equation of ac grids shown in (8), the weights that define the proportion of disturbance sharing among the ac power systems and the droop relation of converters. The ac grids can be represented by (8) for the study of frequency regulation [30].

$$\begin{cases} \Delta\dot{f} &= \dfrac{1}{2H}\left(-D\Delta f + \Delta P_m - \Delta P_L - \Delta P_{agg}^{VSC}\right) \\ \Delta\dot{z} &= -\dfrac{1}{T_{gov}}\Delta z + \dfrac{1}{T_{gov}}G_{gov} - \Delta f \\ \Delta\dot{P}_m &= -\dfrac{1}{T_{CH}}\Delta P_m + \dfrac{1}{T_{CH}}\Delta z \end{cases} \tag{8}$$

where, H is the inertia time constant, D and G_{gov} are the damping and governor droop constant respectively, ΔP_m and ΔP_L are the change in mechanical power and ac load in their respective order. On the other hand, ΔP_{agg}^{VSC} is the aggregated power deviation of converters interfaced to an ac area. T_{gov} is the governor time constant, T_{CH} time constant of the steam chest.

For the case of converter outage, the CFSS has the objective to avoid the frequency deviation by restoring the power flow between the ac and dc grids. Therefore, the dc voltage deviation is expressed as shown in (9). For the same magnitude of aggregated droop gain, the magnitude of dc voltage deviation is smaller in the case of CFSS compared to the conventional $P - V_{dc} - f$ droop control as it is seen from second line of (5) and (9).

$$\Delta V_{dc} = -P_k \frac{1}{G_{v,agg,suv}^{dcDis}} \tag{9}$$

where, $G_{v,agg,suv}^{dcDis}$ is the aggregated droop gain of survivor converters for the operation during converter outage.

However, the CFSS has couple of drawbacks. In design of the droop gains for the case of ac disturbance, the dc grid parameters and the VSCs power losses were neglected. In evaluating its performance, though the CFSS shows better response compared to other mechanisms, the desired disturbance sharing wasn't exactly achieved. Moreover, the power losses of the VSCs weren't included in the modeling of the MTDC system. Also, in reality, the length of transmission lines can be very long, for instance the HVDC cable of the North Sea link has 724km distance [31]. All these can make the impact of dc grid parameters on the performance of the droop gains very high. Therefore, the droop gains won't perform as per their design and there will be disproportional disturbance sharing among the ac grids. In some cases, the malfunctioning of droop gains can cause adverse effect on the frequency of ac grids; particularly those with relatively small size. In addition, the dc voltage during converter outage can be significant as shown in (9); particularly, if the tripped converter was operating at high power. Furthermore, the CFSS didn't study how the ac grids share the stress during windfarm power variation.

III. The Overall Operation Strategy of the Proposed Scheme

As discussed previously, the nature of the impact disturbances impose on the frequency and dc voltage of the ac/dc grid is different. Hence, this work develops the frequency support schemes accordingly for better frequency and dc voltage regulation. For the case of ac disturbance, a supplementary controller is developed to be augmented with the strategy adopted from CFSS. Therefore, the droop gains can function as per the design, and the ac grids share the disturbance according to their size and the specified proportions. During converter outage, the objective of the proposed mechanism is to maintain the dc voltage profile at a level before the disturbance and also minimizing the frequency deviation of the interconnected ac grids. Furthermore, the proposed work formulates a mechanism to make ac grids share the stress due to windfarm power variation according to their size. Fig. 2 shows how a specific converter identifies the type of disturbance and switches its control mode to the corresponding frequency support. As the figure shows, a converter depends on the information of frequency and dc voltage deviation, and communication signals for detecting which disturbance occurs.

A) If a converter senses only frequency deviation, it will understand that ac disturbance happens at its ac grid. This is because during ac disturbance, only the frequency of the disturbed ac grid deviates until the frequency support scheme is activated as discussed in section II-A. Once detecting ac disturbance, a converter will switch its controller to ac disturbed mode of operation (see Fig. 4). Also, converters in other ac grids will be informed by sending a signal with information of the disturbed ac grid and the type of disturbance.

B) On the other hand, if a converter detects both frequency and dc voltage deviation, it can't distinguish the type of disturbance from this information only. The reason is that the simultaneous frequency and dc voltage deviation can be caused by either converter outage or windfarm power variation as it is highlighted in section II-A. Also, a converter can sense the dc voltage and frequency deviation due to the activation of ac disturbed mode of operation ($P-f$ droop control) by remote converters. Therefore, the converter will need to check for any received signal to detect the exact cause of the incidence.

C) If the received signal is for converter outage from the tripped converter, the receiver converter will activate the corresponding frequency support. If the converter is interfaced with the same ac grid as the tripped one, it will operate in mode of operation shown in Fig. 5. Otherwise, it will keep working in the nominal mode of operation. Note that, in the case of converter outage, the tripped converter notifies the survivor ones by transmitting a signal embedding information of itself, its ac grid and the type of disturbance.

D) If the signal is a help request signal for the case of ac disturbance from remote converters, it will activate its supporting mode of operation as depicted in Fig. 3.

E) On the other case, if no signal is received, the converter will keep working in nominal mode of operation. The droop gains in the nominal mode of operation are determined considering the disturbance sharing ratio among ac grids during windfarm power variation.

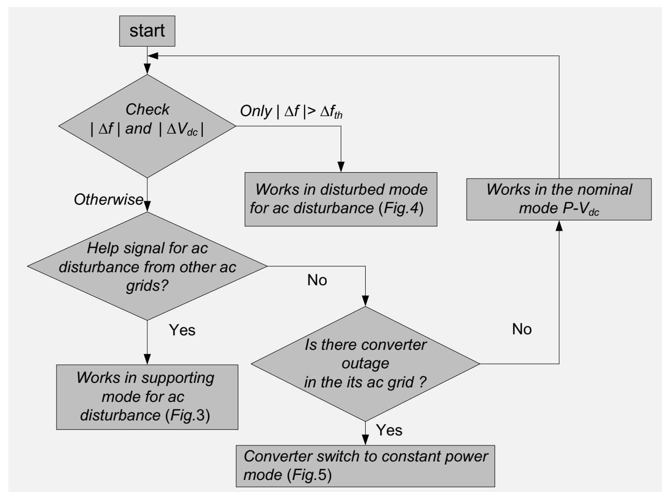

Fig. 2. Flow chart for the proposed mechanism

IV. The Proposed Supplementary Controller

This section presents the development of the supplementary controllers. In all the above equations, a lossless MTDC system was considered. However, from now on, the dc network parameters and the power losses of VSCs will be included in the formulations.

1) Impact of dc grid parameters and power losses of VSCs on performance of the droop gains in CFSS: For the explanation, let us consider three asynchronous ac areas (a_1, a_2 and a_3) interconnected by MTDC system. Also, it is assumed that the ac contingency occurs at area a_3. Moreover, at steady-state (for the study of primary frequency response), (8) can be simplified to (10).

$$\mathbf{M\Delta f} + \mathbf{\Delta P_{agg}^{VSCs}} = \mathbf{\Delta P_L} \tag{10}$$

where, $\mathbf{\Delta P_{agg}^{VSCs}} = \begin{bmatrix} \Delta \mathrm{P}_{agg,a_1}^{VSCs} & \Delta \mathrm{P}_{agg,a_2}^{VSCs} & \Delta \mathrm{P}_{agg,a_3}^{VSCs} \end{bmatrix}^T$,

$\mathbf{\Delta f} = \begin{bmatrix} \Delta \mathrm{f}_{a_1} & \Delta \mathrm{f}_{a_2} & \Delta \mathrm{f}_{a_3} \end{bmatrix}^T$, $\mathbf{\Delta P_L} = \begin{bmatrix} 0 & 0 & \Delta \mathrm{P}_L \end{bmatrix}^T$

This article has been accepted for publication in IEEE Transactions on Power Systems. This is the author's version which has not been fully edited and content may change prior to final publication. Citation information: DOI 10.1109/TPWRS.2023.3279364

$$\mathbf{M}=\begin{bmatrix} \mathrm{D}_{a_1}+\mathrm{G}_{gov,a_1} & 0 & 0 \\ 0 & \mathrm{D}_{a_2}+\mathrm{G}_{gov,a_2} & 0 \\ 0 & 0 & \mathrm{D}_{a_3}+\mathrm{G}_{gov,a_3} \end{bmatrix}$$

$$\Delta P_{agg,a_1}^{VSCs}=\sum_{j\in\phi^{a_1}} g_{v,j}^{sup}\Delta V_{dc,j}\ ,\ \Delta P_{agg,a_3}^{VSCs}=G_{f,agg}^{dis}\Delta f_{a_3}.$$

If we consider the supporting ac areas i.e. area a_1 and a_2, the relation in (11) can be obtained after some manipulation. It can be observed that the proportion that ac grids share the disturbance depends on the dc voltage deviations of the converters. Therefore, if the converters dc voltage deviations are too different, there will be disproportional sharing of disturbance. For instance, if the dc voltage deviation of converters interfaced to ac grid #1 is much higher, the frequency deviation of area #1 will be more than that of ac grid #2 though the droop gains are designed to make area #1 carry less burden than area #2.

$$\frac{\Delta f_{a_1}}{\Delta f_{a_2}}=\frac{\sum\limits_{j\in\phi^{a_1}} g_{v,j}^{sup}\Delta V_{dc,j}}{D_{a_1}+G_{gov,a_1}}\frac{D_{a_2}+G_{gov,a_2}}{\sum\limits_{j\in\phi^{a_2}} g_{v,j}^{sup}\Delta V_{dc,j}} \tag{11}$$

Furthermore, the power balance in the MTDC system is governed by (12).

$$\Delta P_{loss}=\Delta P_{agg,a_1}^{VSCs}+\Delta P_{agg,a_2}^{VSCs}+\Delta P_{agg,a_3}^{VSCs} \tag{12}$$

Therefore, for area #3, the expression in (13) is found after substituting (12) into (10), and doing some rearrangement. It can be seen that the performance of the droop gain depends on the power losses of the system.

$$G_{f,agg}^{dis}\Delta f_{a_3}=\Delta P_{loss}+\sum_{a_j\in a_1\cup a_2}\left(D_{a_j}+g_{gov,a_j}\right)\Delta f_{a_j} \tag{13}$$

Therefore, in this work, supplementary controllers for both supporting and disturbed modes are proposed to mitigate the impact of the dc network parameters and VSCs power losses. A general ac/dc power system with n number of converters and m ac areas is considered.

2) Supplementary controller for the supporting mode: The structure of the proposed mechanism is described in Fig. 3. It is developed based on the ideal case that the dc grid and converters are lossless. Hence, considering all the converters in the supporting mode, the ideal dc voltage deviation can be obtained as (14).

$$\Delta V_{dc}^{desired}=\frac{1}{\sum\limits_{a_k\in\zeta}\sum\limits_{j\in\phi^{a_k}} g_{v,j}^{sup}}\sum_{a_k\in\zeta}\sum_{j\in\phi^{a_k}}\Delta P_j \tag{14}$$

where, $\Delta P_j=P_j-P_{ref,j}$, ϕ^{a_k} is the set of converters in the undisturbed ac power system a_k. ζ is the set of ac grids in the supporting mode. The objective of the supplementary controller is to add compensation term to the dc voltage deviation of each converter to obtain $\Delta V_{dc}^{desired}$ at steady-state.

$$\Delta V_{dc}^{desired}=V_{dc,ref,j}-V_{dc,j}-\Delta V_{dc,j}^{compn},\ \ j\in\phi \tag{15}$$

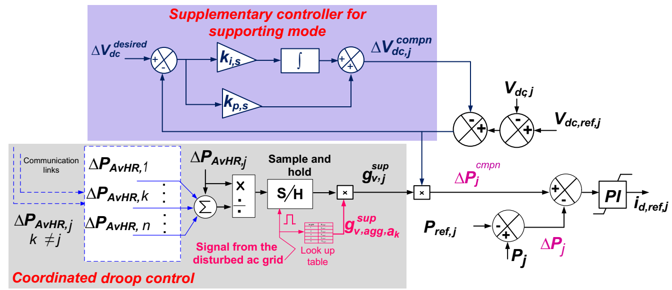

Fig. 3. Proposed supplementary control mechanism for supporting mode

Moreover, $\Delta V_{dc}^{desired}$ is used in the dc voltage droop control of converters as Fig. 3 shows to generate a compensation term ($\Delta P_j^{compn}=g_{v,j}^{sup}\Delta V_{dc}^{desired}$) added to the power reference of converters in the supporting mode. On the other hand, the active power controller make sure that ΔP_j^{compn} and ΔP_j are equal at steady-state. Also, since the active power controller is much faster than the electromechanical transients of the ac grids, its dynamics can be ignored, and ΔP_j^{compn} can be taken as equal to ΔP_j. Therefore, the actual active power deviation of converters in each supporting ac area can be expressed as shown in (16).

$$\begin{cases}\Delta P_j & =g_{v,j}^{sup}\Delta V_{dc}^{desired}\\ \Delta P_{agg,a_k}^{VSCs} & =\Delta V^{desired}G_{v,agg,a_k}^{sup}\end{cases} \tag{16}$$

where, $G_{v,agg,a_k}^{sup}=\sum\limits_{j\in\phi^{a_k}} g_{v,j}^{sup}$. If the second line in (16) is used in (11) for the sum of power change of converters in each supporting ac power system, the relation between the frequency deviation of the ac grids in any two supporting areas can be obtained as shown in (17).

$$\frac{\Delta f_{a_1}}{\Delta f_{a_2}}=\frac{G_{v,agg,a_k}^{sup}}{D_{a_k}+G_{gov,a_k}}\frac{D_{a_l}+G_{gov,a_l}}{G_{v,agg,a_l}^{sup}} \tag{17}$$

It can be seen that the relation among the frequency deviation of ac grids depends only on the designed droop gains and size of the ac grids. The droop gains are designed considering the specified proportion that ac grids share the disturbance. The reader can refer to [23] for the details of designing the droop gains.

In Fig. 3, $\Delta P_{AvHR,k}$ is the available headroom of a converter. Moreover, a lookup table is included in the control system. For MTDC system interconnecting n ac areas, converters will have $n-1$ different droop gains for supporting case, and one frequency droop gain for the disturbed mode. For instance, if consider the hybrid ac/dc system with the three areas (a_1, a_2 and a_3), the value of the supporting mode droop constants of converters in area a_1 are different for the case of ac contingency in area a_2 and a_3. Hence, each converter will have a look up table as Fig. 3 describes. The converters select the appropriate supporting mode droop constant based on the received signal.

3) Supplementary control for the disturbed mode: In this part, the proposed supplementary control for the case of disturbed mode will be discussed. Similar to the case of the supporting mode, the controller is developed considering the ideal condition. Therefore, the frequency deviation of the

This article has been accepted for publication in IEEE Transactions on Power Systems. This is the author's version which has not been fully edited and content may change prior to final publication. Citation information: DOI 10.1109/TPWRS.2023.3279364

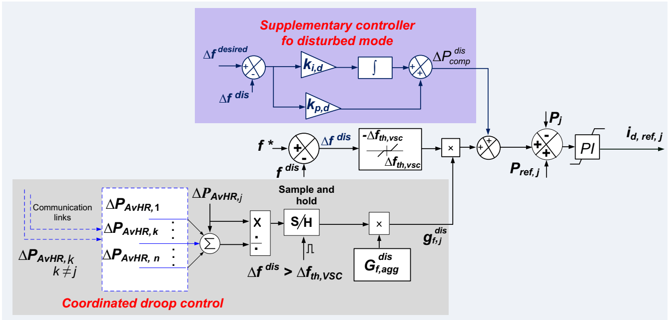

Fig. 4. Proposed supplementary control mechanism for disturbed mode

perturbed area in ideal condition can be written as shown in (18) after putting ΔP_{loss} zero in (13).

$$\Delta f^{desired} = \frac{\sum\limits_{a_k \in \zeta} \sum\limits_{j \in \phi^{a_k}} \Delta P_j}{G^{dis}_{f,agg}} \tag{18}$$

In the proposed supplementary controller, the expression in (18) is used as a reference as it is depicted in Fig. 4. At steady-state, the power balance of the MTDC system considering the supplementary controllers can be expressed as shown in (19).

$$\sum_{a_k \in \zeta} \Delta P^{VSCs}_{agg,a_k} + G^{dis}_{f,agg} \Delta f^{dis} + \Delta P^{dis}_{comp} = \Delta P_{loss} \tag{19}$$

where, Δf^{dis} is the frequency perturbation of the disturbed area. However, the supplementary controller for the disturbed mode makes sure that $\sum\limits_{a_k \in \zeta} \Delta P^{VSCs}_{agg,a_k} = -G^{dis}_{f,agg} \Delta f^{dis}$. Therefore, the output of the supplementary controller in the disturbed mode is to compensate for the dc grid and VSCs power losses as $\Delta P^{dis}_{comp} = \Delta P_{loss}$. Moreover, the expression for the power deviation of converters interfaced to disturbed ac grid shown in (10) can be changed to (20) considering the supplementary controller. Note the term Δf_{a_3} is replaced by Δf^{dis} for a general system.

$$\Delta P^{VSCs,dis}_{agg} = G^{dis}_{f,agg} \Delta f^{dis} + \Delta P^{dis}_{comp} \tag{20}$$

Hence, combining (10), (16), (19), (20) and $\Delta P^{dis}_{comp} = \Delta P_{loss}$ yields the expression for the relation between the frequency deviation of the affected are and the supporting ac grids as depicted in (21). It is shown that the droop gains perform independent of the power losses unlike the one shown in (13). The detail procedure of calculating the frequency droop gain based on the specified weights that establish the disturbance sharing among the ac grids is presented in [23].

$$G^{dis}_{f,agg} \Delta f^{dis} = \sum_{a_k \in \zeta} \left(D_{a_k} + g_{gov,a_k}\right) \Delta f_{a_k} \tag{21}$$

For realizing the supplementary controllers, converters interfaced to the undisturbed ac areas should exchange the information of their power deviation, ΔP_j, to each other and also share the information to converters in the disturbed mode. However, the existing communication network and signals used for coordination can be employed. For the adaptive droop gain mechanism, converters that are neighbors to the ac side share the information of their available headroom. Therefore, if a converter knows the scheduled power ($P_{scheduled,x}$) and the maximum capacity ($P_{max,x}$) of other converters, the power deviation of those converters can be determined as depicted in (22). Consequently, converters in the same supporting ac area don't need to exchange the information of their power deviation. This can reduce the burden of the communication network. However, converters in different supporting ac grids should communicate the calculated power deviation. Furthermore, the proposed supplementary controller can work with a low bandwidth communication network. As it was discussed above, the purpose of the mechanism is to make sure the designed droop gains achieve the desired performance at steady-state. The main frequency support is facilitated by the designed droop gains based on the adaptive scheme. Therefore, the supplementary controller has slow speed and can work in low bandwidth communication network.

$$\begin{cases} \Delta P_{AvHR,x} & = P_{max,x} - P_x \\ \Delta P_x & = P_{max,x} - \Delta P_{AvHR,x} - P_{scheduled,x} \end{cases} \tag{22}$$

where, $\Delta P_{AvHR,x}$ is the available headroom and P_x is the present loading of a converter.

V. Nominal Droop Gains Design

The power output of the wind farm is not constant due to the variable wind speed. Therefore, there should be a mechanism to handle the disturbance to ease the impact on the frequency deviation of the ac grids. The proposed disturbance sharing mechanism among ac grids during offshore wind farm power variation depends on the design of the nominal dc voltage droop gains. Moreover, to mitigate the impact of the dc grid and VSCs power losses on the performance of the designed droop gains, a supplementary controller similar to the supporting mode in the case of ac disturbance is developed. Therefore, in the following discussions, the steps of designing the droop constants are presented according to the ideal conditions.

The power change in each ac grid because of the wind farm power variation was discussed in section II-A3. Therefore, the swing equation can be rewritten as shown in (23) for n ac grids considering the power deviation of ac grids due to windfarm power deviation. In addition, the disturbance sharing percentages among the ac grids defined in terms of the ratio ($\Delta f_{a_1} : \cdots : \Delta f_{a_n} = w_{a_1} : \cdots : w_{a_n}$) between their frequency deviation is included in (23).

$$\mathbf{M} \Delta f_{c_n} + \mathbf{F} \Delta P_{wf} = 0 \tag{23}$$

where,

$$\mathbf{M} = \mathbf{CR}, \mathbf{R} = \begin{bmatrix} \frac{w_{a_1}}{w_{a_n}} & \cdots & \frac{w_{a_k}}{w_{a_n}} & \cdots & 1 \end{bmatrix}^T$$
$$\mathbf{C} = \mathbf{diag}\left(-(D_{a_1} + g_{gov,a_1}), \cdots, -(D_{a_n} + g_{gov,a_n})\right)$$
$$\mathbf{F} = \begin{bmatrix} \frac{G^{nom}_{v,agg,a_1}}{G^{nom}_{agg}} & \cdots & \frac{G^{nom}_{v,agg,a_k}}{G^{nom}_{agg}} & \cdots & \frac{G^{nom}_{v,agg,a_n}}{G^{nom}_{agg}} \end{bmatrix}^T$$

If we sum all the rows of (23), we obtain (24).

$$\Delta P_{wf} = \Delta f_{a_n} \sum_{a_k \in S^{acGrid}} \left(D_{a_k} + g_{gov,a_k}\right) \frac{w_{a_k}}{w_{a_n}} \tag{24}$$

This article has been accepted for publication in IEEE Transactions on Power Systems. This is the author's version which has not been fully edited and content may change prior to final publication. Citation information: DOI 10.1109/TPWRS.2023.3279364

Substituting (24) into (23) for ΔP_{wf} yields:

$$\mathbf{M} + \mathbf{FKR} = 0 \tag{25}$$

where, $\mathbf{K} = \begin{bmatrix} -(D_{a_1} + g_{gov,a_1}) & \cdots & -(D_{a_n} + g_{gov,a_n}) \end{bmatrix}$. Therefore, the dc voltage droop gains (elements of matrix $\mathbf{F}$) can be determined from (25). Moreover, since the matrix isn't full rank, there are number of solutions for the droop gains.

However, there is also other constraint on the magnitude of these droop gains related to the dc voltage deviation. As it was discussed in section III, when converter outage occurs, survivor converters will switch their control strategy for the case of converter outage. However, it takes some time till the converters transit to this control mode due to the communication delay. Therefore, for short period of time, the system works in nominal operation though there is incidence of converter outage. Note that this is also the same for the case of ac disturbance. However, converter outage has more significant impact on the dc voltage deviation than ac disturbance. As a result, the nominal droop gains have to be designed considering the permissible dc voltage deviation during converter outage. For this, the constraint is taken considering that a converter with the highest power rating trips while it works at its rated power as it is discussed in [33]. Therefore, the total droop gain of converters in area a_m can be written as shown in (26).

$$G^{nom}_{v,agg,a_m} = \frac{w_{a_m}(D_{a_m} + g_{gov,a_m})}{\sum\limits_{a_k \in S^{acGrids}} (D_{a_k} + g_{gov,a_k})\, w_{a_k}} \frac{\max\limits_{j \in S^{VSCs}} (P_{rated,j})}{\Delta V_{dc,max}} \tag{26}$$

where, S^{VSCs} is set of converters, $P_{rate,j}$ is the rated power of converters and $\Delta V_{dc,max}$ is the peak tolerable dc voltage deviation during the considered worst contingency.

VI. The Proposed Strategy for Converter Outage

The objective of the proposed scheme is to alleviate the consequence of converter tripping on the dc voltage and frequency of the hybrid power system. Hence, a new mechanism is developed to transfer the loading of the tripped converter prior to the incidence to the survivor ones. During converter outage, the survivors that are ac neighbors of the tripped converter operate in constant power mode depicted in Fig. 5. Moreover, these converters modify their power reference according to the power of the tripped converter before the event and their available headroom. For this purpose, they inform each other about the magnitude of their available capacity. In addition, the tripped converter sends the information of its operating power before the incidence to its ac neighbors. On the other hand, the converters in the other ac power systems will keep their nominal dc voltage droop control mode of operation. The power balance of MTDC system in the proposed strategy can be written as shown in (27).

$$\begin{aligned} \Delta P^{tripped}_{VSC} &+ \sum_{j \in \phi^{healthy}} k_{v,j} \Delta V_{dc,j} \\ &+ \sum_{j \in \phi^{disDC}} \Delta P_j = \Delta P_{loss} \end{aligned} \tag{27}$$

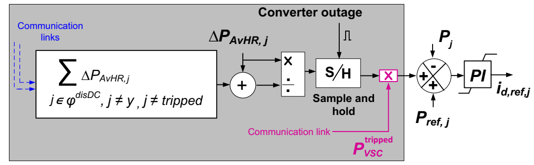

Fig. 5. Proposed mechanism for the survivor and ac neighbor of the tripped converter

where, the set ϕ^{disDC} has converters that are ac neighbors of the tripped converter and ΔP_j is their power deviation, $\phi^{healthy}$ is the set of converters in the other ac power systems, and $\Delta V_{dc,j}$ and $g_{v,j}$ are their dc voltage and droop gains accordingly, $\Delta P^{tripped}_{VSC}$ is the tripped converters' power change. However, the power deviation of the tripped converter will be equal to the magnitude of the total power change of its ac neighbors.

$$\Delta P^{tripped}_{VSC} = - \sum_{j \in \phi^{disDC}} \Delta P_j \tag{28}$$

In (28), it is assumed that the total available capacity of the survivor converters is equal or greater than the loading of the tripped converter prior to the event. Using (28), the expression in (27) can be reduced to:

$$\sum_{j \in \phi^{healthy}} k_{v,j} \Delta V_{dc,j} = \Delta P_{loss} \tag{29}$$

From (29), it is observed that the dc voltage is affected only by the power losses. The impact of the power unbalance due to the tripped converter on the dc voltage response is avoided. However, in CFSS [23], the dc voltage deviation depends on the load of the tripped converter prior to the incidence as shown in (9). Note that in (9), the analysis is based on the assumption of lossless MTDC system. Furthermore, the deviation of the power transmission between the dc network and each ac area can be minimized. For instance, (30) depicts the power change in the ac area with the tripped converter. It can be seen that the deviation of the power flow between the ac and dc systems is zero.

$$\Delta P^{disAcGrid} = \sum_{j \in \phi^{dis}} \Delta P_j + \Delta P^{tripped}_{VSC} = 0 \tag{30}$$

where, $\Delta P^{disAcGrid}$ is the deviation in the power flow between the ac system with the tripped converter and the dc grid. For the other ac grids, the power change will be expressed as shown in (31).

$$\Delta P^{healthyAcGrid}_{a_k} = \sum_{j \in \phi^{healthy,a_k}} k_{v,j} \Delta V_{dc,j} \tag{31}$$

where, $\phi^{healthy,a_k}$ is the set of converters in ac power systems that don't have the tripped converter. The change in the power flow between these ac areas and the dc grid is associated with only the power losses as it can be observed from the combination of (29) and (31). In other word, the drift in the frequency of these ac power systems is related to only the power losses when converter tripping occurs.

VII. Case studies

For verifying the proposed mechanism, the model of an ac/dc power system has been developed in Matlab/Simulink. Fig. 6 shows the schematics of the test system. The IEEE 68 bus model is modified to form three asynchronous ac power systems interconnected by 8-terminal MTDC system. Also, an offshore windfarm is included in the system. The model of the MTDC system is developed considering the average value of converters, the admittance matrix of the dc grid and different controllers of the converters. The details on modeling of MTDC system are presented in [32]. Moreover, the VSCs' power losses are considered, and a mechanism reported in [34] is used to model these power losses. In this work, the offshore wind farm is operating at its maximum power point. A threshold value of ±36mHz is considered for the frequency support mechanism [35]. A communication topology similar to the one reported in [23] is used, and the communication lines are assumed to have the delays depicted in Table I. Furthermore, the test cases are established to assess the performance of the proposed scheme during the occurrence of different disturbances such as ac disturbance, converter outage and wind farm power deviation.

TABLE I
Approximate time delay of communication links

lines	delay (sec.)	lines	delay(sec.)
1-6	0.275	4-7	0.3
1-8	0.3	5-6	0.325
3-4	0.225	6-7	0.25
4-5	0.25	7-8	0.26

TABLE II
Relevant parameters of ac grids

ac grids	D(p.u.)	$g_{f,gov}(p.u.)$
1	77.5	26
2	300	70
3	98.66	34

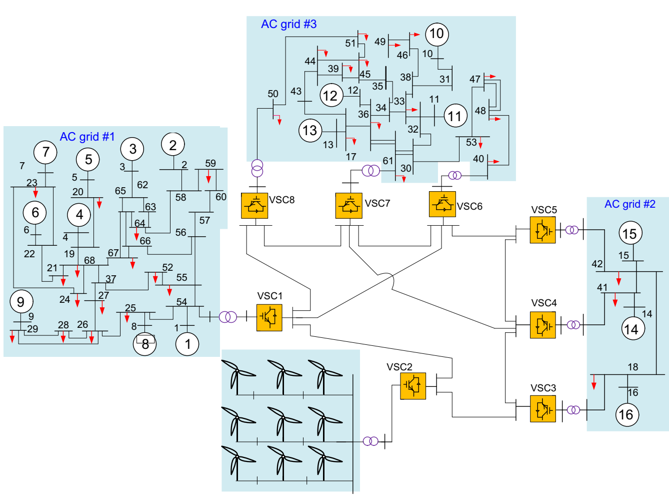

Fig. 6. Schematic diagram of the test system

A. Impact of control parameters on the small signal stability of the system

Before going to the time domain simulation results and discussion, this subsection aims to present how the droop gains and the gains of the supplementary controller affect the small signal stability of the system briefly. The Matlab linearization toolbox is used to get the state space representation of the test system.

1) Eigenvalues with variation of droop gains for the case of ac disturbance: The droop gains are varied in pairwise since they are determined to satisfy the specified disturbance sharing proportions among the ac grids. The steps of calculating the droop gains can be found in [23]. The values are obtained considering ac disturbance at area #3 of the test system. The aggregated frequency droop gain (473.75 p.u. or 789.3MW/Hz) for disturbed mode is constant for a given weights ($\Delta f_1 : \Delta f_2 : \Delta f_3 = 1 : 1 : 1$). Therefore, the variation is conducted on the droop gains of converters in the unaffected areas. The small signal model has total of 227 eigenvalues; however, the variation of the droop gains affects only some of them. Fig. 7 depicts the movement of the affected eigenvalues as the droop gains vary from (10, 35.66) in p.u. or (1.56MW/kV, 5.57MW/kV) to (800, 2852.8) in p.u. or (125W/kV, 445.7875MW/kV) in the interval of (10, 35.66) in p.u. or (1.56MW/kV, 5.57MW/kV). Moreover, the movement of the poles isn't uniform. Some of them (λ_{93}, λ_{94}, λ_{104}, λ_{105}, λ_{106} and λ_{107}) move to the left. However, there are others (λ_{11}, λ_{12}, λ_{13} and λ_{14}) that migrate towards right as the droop gains increase.

From the analysis, it is shown that a very large droop gain can cause the eigenvalues move to the right half plane. On the other hand, small droop gain will have impact on the dc voltage deviation during frequency support. Although the structure of the droop control in our proposed scheme ($P-f$ for converters in the disturbed area and $P-V_{dc}$ for converters in the undisturbed ac power systems) have better decoupling between dc voltage deviation and frequency support compared to other mechanisms, the dc voltage deviation still depends on the dc voltage droop gain of the $P-V_{dc}$ droop controlled converters. Therefore, the selection of droop gains should consider this trade off.

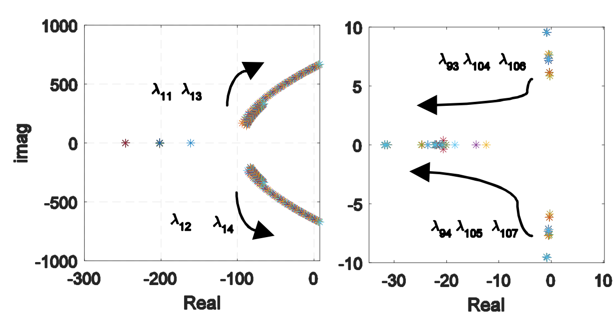

Fig. 7. Eigenvalues trajectory when the droop gains vary

2) Eigenvalues with variation of the supplementary controller gains: The movement of the eigenvalues is studied by varying the integral gains of the supplementary controllers.

The proportional gain can be set to zero since the objective of the supplementary controller is for correction at steady-state. Fig. 8 a) depicts the migration of the most affected eigenvalues when the integral gain of the supplementary controller for the supporting mode varies from 0.5 p.u to 100 p.u. Eigenvalues $\lambda_{11,12}$, $\lambda_{13,14}$, $\lambda_{18,19}$ and $\lambda_{20,21}$ move to the left. This indicates that the supplementary controller increase the damping constant of the eigenvalues. On the other hand, the change in the value of the integral gain of the disturbed mode supplementary controller doesn't have noticeable impact on the location of the eigenvalues. For the reference, the movement of the eigenvalues λ_{18}, λ_{19}, λ_{20} and λ_{21} is shown in Fig. 8 b). From the analysis, increasing the integral gain of the supplementary controller for the supportive mode makes the eigenvalues to shift more to the left. However, the controller doesn't need to be aggressive as the change in operating condition can alter the motion of the eigenvalues. Moreover, it is the steady state performance of the controller that is the most desirable. Therefore, lower gain value can be chosen.

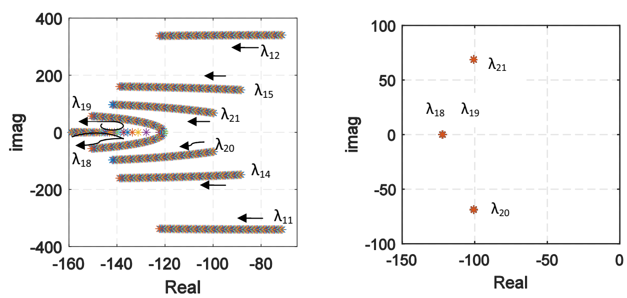

(a) (b)

Fig. 8. Eigenvalues movement with the variation of the integral gain of supplementary controllers (a) supporting mode (b) disturbed mode

B. Assessment of the proposed supplementary controllers

In this subsection, the proposed scheme is assessed during ac disturbance. To simulate the ac disturbance, the load at bus #61 in ac grid #3 increase by 500MW (5p.u. or 8.2% of original load) at time $t = 3s$. The gains for the supplementary controllers are selected considering the small signal analysis of the ac/dc system. Accordingly, the integral gains for the supporting mode supplementary controller are 10 p.u., and for the disturbed mode they have values of 10 p.u. Moreover, the weights are defined to be $\Delta f_1 : \Delta f_2 : \Delta f_3 = 1 : 1 : 1$. Therefore, the values of the combined droop constants of converters in each ac area are 200pu (31.24MW/kV), 713.25pu (111.4453MW/kV) and 473.75 pu (789.5833MW/Hz) respectively. Since the ac disturbance happens at area #3, the converters in this area operate in disturbed mode and those in ac power system #1 and #2 work in supporting mode. The proposed technique is compared to the existing mechanisms CFSS [23] and [20].

1) Frequency deviation: As Fig. 9 shows, the proposed scheme achieves the specified disturbance-sharing proportion among the interconnected areas. The three ac grids have the same frequency deviation of 0.51Hz at steady state. However, in [23], the ac power systems have different frequency deviation as the dashed lines in Fig. 9 a) illustrates. The three ac grids have 0.83, 0.45 and 0.49 Hz accordingly. Bear in mind that, for the specified ratio, the droop gains in [23] have the same values as the proposed technique. Also, similar to the proposed mechanism, [23] has coordinated droop gain scheme for individual converters. However, the impact of the dc grid and VSCs power losses isn't considered. Therefore, the designed droop gains can't provide their anticipated performance.

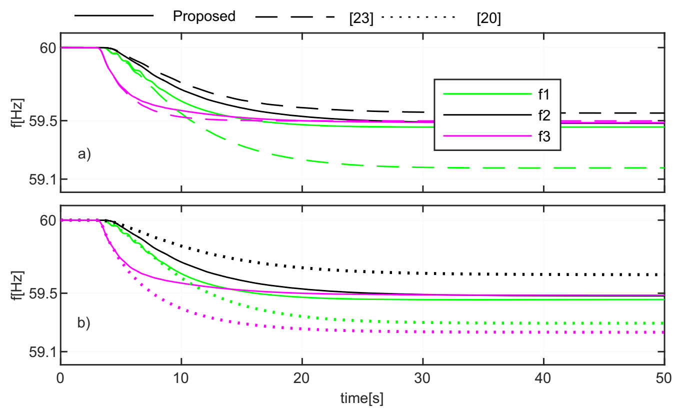

Fig. 9. Frequency response when the load of area #3 increases by 5p.u. (500MW) a) Proposed vs [23] b) Proposed vs [20]

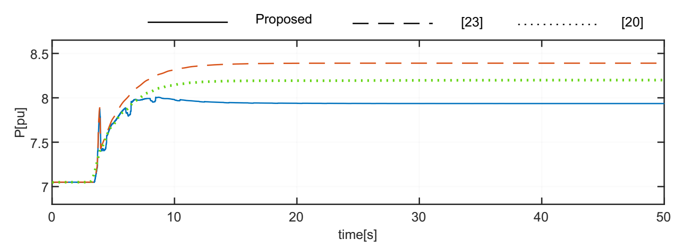

Fig. 10. Power response of converter #1 when the load at area #3 increases by 5p.u. (500MW)

In the proposed strategy, the supplementary controllers add the correction terms to the coordinated droop scheme to mitigate the effect of dc grid and VSCs power losses. Hence, the supplementary controller for converters in the supporting mode makes them share the burden based on their droop gains. As a consequence, those in the same supporting ac grid have power deviation proportional to their available capacity since, in the coordinated droop gain scheme, the converters determine their droop gain based on how much vacant room they have. For instance, if we consider converters #3, #4, and #5 in area #2, their loading are changed by 0.164, 0.62, and 2.379 p.u. respectively as the solid lines in Figs. 11 a) and b) depict. If we determine the ratio of the power changes, it will be $1 : 3.76 : 14.56$, the same as the ratio among the converter's available capacity (see Table III). Moreover, converters in different supporting ac areas share the burden according to their droop gain. Hence, the ratio $(0.89/3.163)$ between the power deviation of converter #1 (see the solid lines in Fig.10) in ac area #1 and converters in ac system #2 is equal to the ratio $(200/731.25)$ between the designed aggregated droop

This article has been accepted for publication in IEEE Transactions on Power Systems. This is the author's version which has not been fully edited and content may change prior to final publication. Citation information: DOI 10.1109/TPWRS.2023.3279364

gains. This implies that (17) is valid in the proposed scheme. However, in the case of [23], the ratio of loading change of converter #1 in area #1 and converters in area #2 is $1.341/2.734$ different from $200/731.25$. Also, the disturbance sharing (0.17, 0.66, and 1.9 p.u) among converters #3, #4, and #5 isn't according to their available capacity. Hence, the coordinated droop gain scheme in [23] can't achieve effective usage of the available capacity of converters. For the case of the converters in ac system #3, Figs. 11 c) and d) show their power response. As the solid lines describe, in the proposed scheme, converters #6, #7, and #8 have the loading change of 0.13, 0, and 3.84 p.u. in the respective order. The ratio of the power deviations is according to their available capacity. Similarly, in the case of [23], the power-sharing (0.135, 0, and 3.89 p.u) is according to the vacant space of converters. Since the converters in area #3 operate in $P-f$ droop control, their power-sharing isn't impacted by the unequal dc voltage deviation. However, there is a difference in the power deviation of these converters in the proposed strategy and [23]. In the former, the supplementary controller for the disturbed mode adds a compensation term for the dc side power losses.

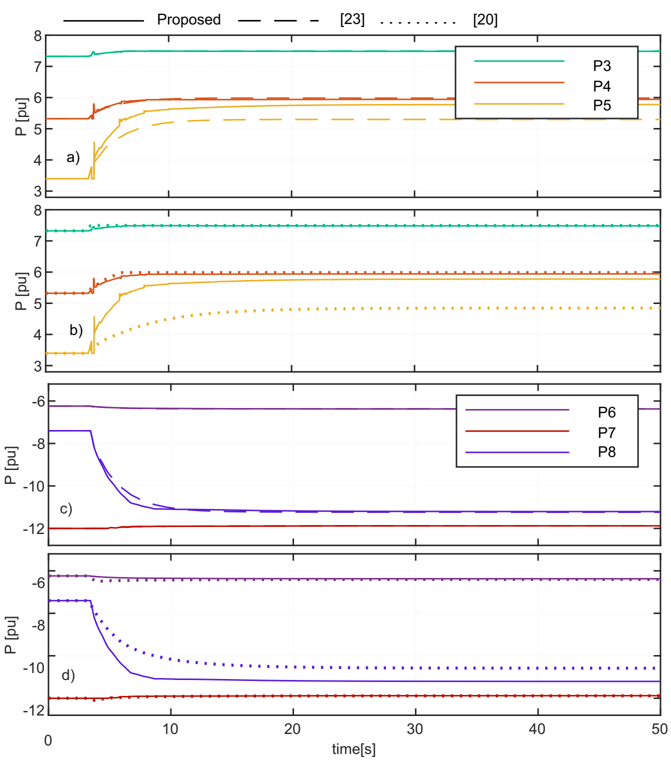

Fig. 11. Power response when the load at area #3 increases by 5p.u. (500MW) a) Proposed vs [23] for converters 3-5 b) Proposed vs [20] for converters 3-5 c) Proposed vs [23] for converters 6-8 d) Proposed vs [20] for converters 6-8

The scheme reported in [20] can't reach at the specified weights between the frequency deviation of the three ac areas. In the respective order, each ac grid has frequency deviations of 0.705, 0.373, and 0.767Hz. In [20], converters operate in $P-V_{dc}-f$ droop control and the frequency droop gains are determined to make ac grids share the burden according to the defined weights. However, there isn't coordination among converters to efficiently use their available capacity. Therefore, when there are converters loaded at their rated capacity, the burden at the time of frequency support can't be rerouted to other converters with more vacant space. For example, considering converters in area #2, the power response of converter #5 (see the dotted line in Fig. 11 b) is small though the converter still has available headroom. The reported mechanism adopts the pilot voltage droop control to mitigate the impact of the dc network parameters. However, the pilot dc voltage droop control depends on fast communication system for stable operation. Regarding the parameter settings, the frequency droop constants are determined to be 132, 90 and 1264 for each ac grid respectively to achieve the same defined weights as that of the proposed scheme. Also, for reasonable comparison, the aggregated dc voltage droop gain is set to be equal to our mechanism.

2) dc voltage deviation: Fig. 12 depicts the dc voltage profile of converters. The proposed mechanism and the strategy in [23] has small dc voltage deviation except insignificant difference between them due to the adjustment by supplementary controllers in the proposed mechanism. However, in [20], the drift in the dc voltage is larger.

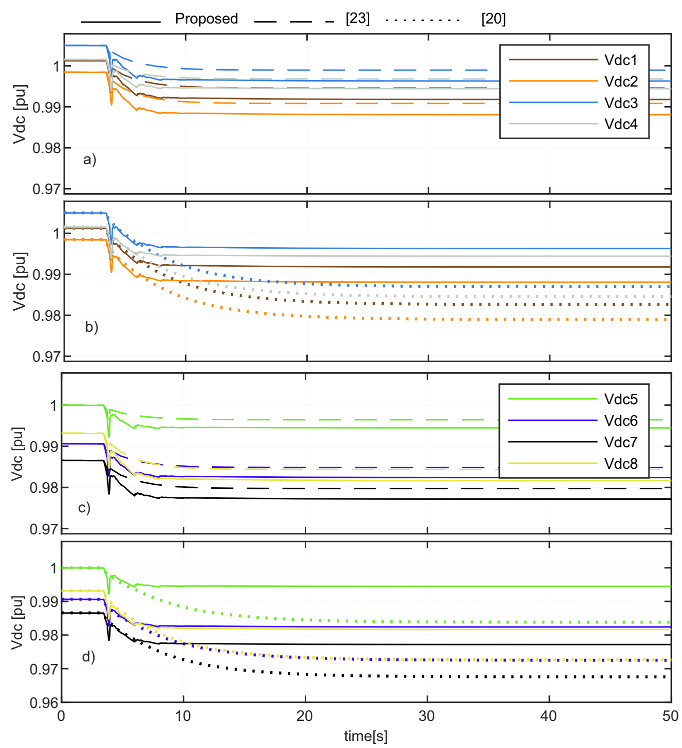

Fig. 12. Converters' dc voltage profile when the load at area #3 increases by 5p.u. (500MW) a) Proposed vs [23] for converters 1-4 b) Proposed vs [20] for converters 1-4 c) Proposed vs [23] for converters 5-8 d) Proposed vs [20] for converters 5-8

C. frequency response during windfarm power deviation

The nominal aggregated droop constants are determined following the specified weights $\Delta f_1 : \Delta f_2 : \Delta f_3 = 1 : 1 : 1$ during the windfarm power deviation. Also, a maximum permissible dc voltage deviation of $\pm 5\%$ during the worst dc disturbance is considered in the design of the droop constants. Therefore, the aggregated droop gains have the values of 51.32 pu (8.02 MW/kV), 183.04 pu (28.6 MW/kV) and 65.63 pu (10.25 MW/kV) for converters in each ac area. Fig.13 shows

This article has been accepted for publication in IEEE Transactions on Power Systems. This is the author's version which has not been fully edited and content may change prior to final publication. Citation information: DOI 10.1109/TPWRS.2023.3279364

TABLE III
RELEVANT PARAMETERS OF VSCS

VSC	Rated power (p.u.)	Operating power (p.u.)	Aailable capacity (p.u.)
1	10	7.05	2.95
3	7.5	7.32	0.18
4	6	5.32	0.68
5	6	3.43	2.57
6	6.5	6.24	0.26
7	12	12	0
8	15	7.4	7.6

the frequency response of the three areas when the power output of the windfarm falls from 445MW to 260MW. The frequency deviation is according to the specified weights. Each ac area has the same frequency deviation of 0.18Hz. For comparison, the performance of [4] is also examined. In [4], the frequency of area #3 deviates by 0.43Hz while the frequency deviation of ac system #2 is 0.1Hz. Hence, the technique in [4] can't make the ac grids share the disturbance according to their strength. The damping ratio and governor droop constant of ac grids are shown in Table II.

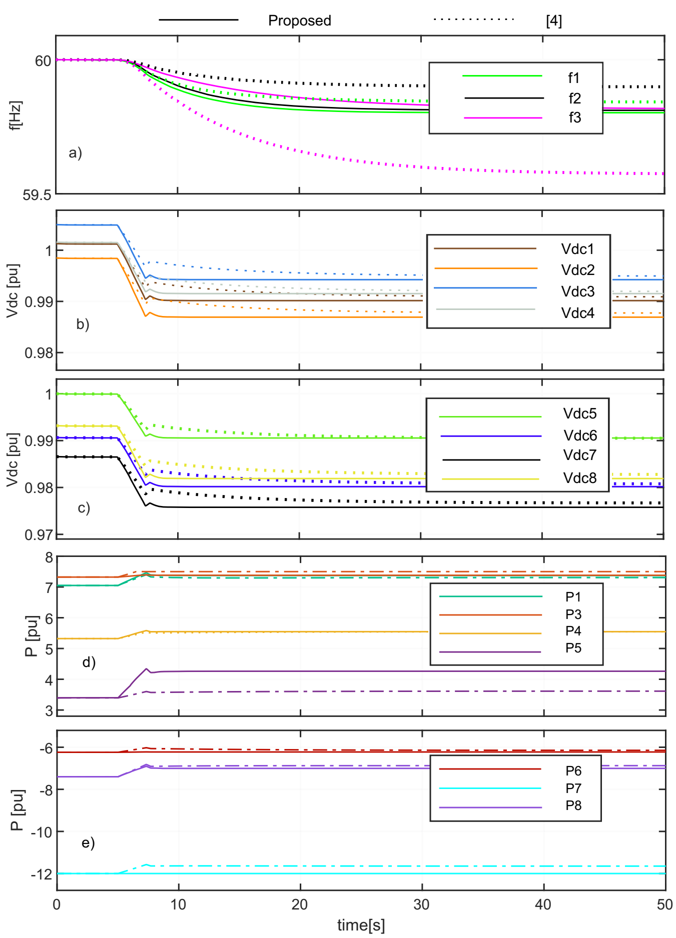

Fig. 13. Responses during windfarm power variation Proposed vs [4] (a) ac grids frequency response (b) dc voltage response (c) converters power response

D. Performance assessment during converter outage

In this subsection, the performance of the proposed mechanism for the case of converter tripping will be discussed. Converter #6 of area #3 is suddenly lost at $t = 10s$. The converter operated at 6.24 p.u. before the incidence.

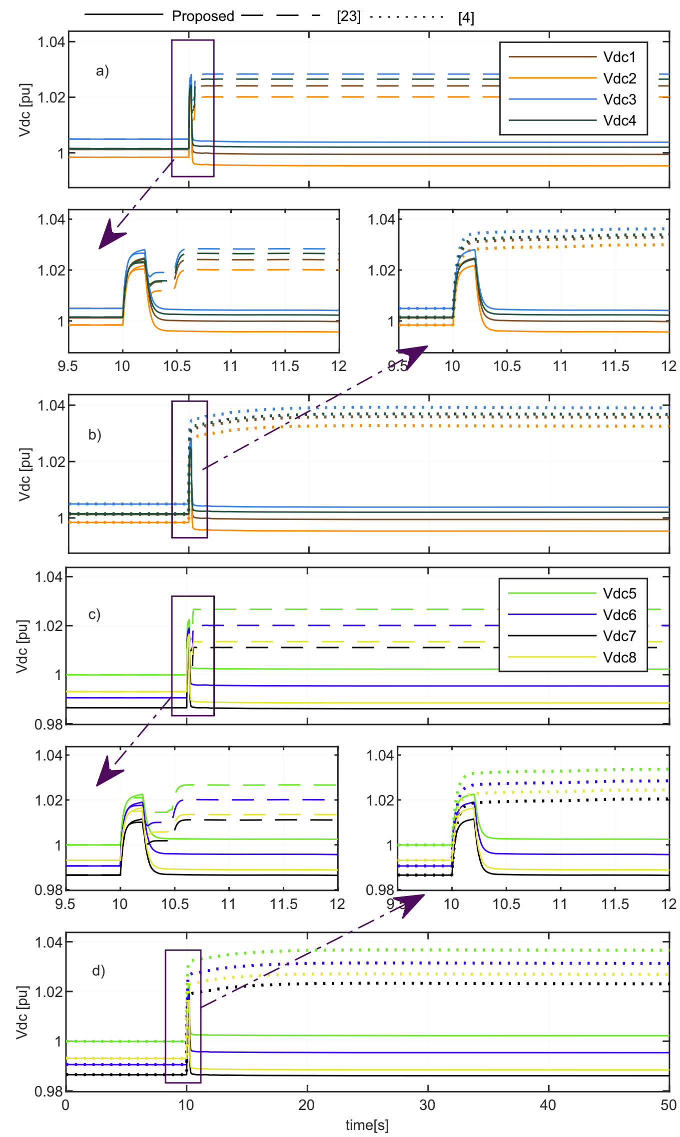

Fig. 14. Converters' dc voltage profile when converter #6 in area #3 trips a) Proposed vs [23] for converters 1-4 b) Proposed vs [4] for converters 1-4 c) Proposed vs [23] for converters 5-8 d) Proposed vs [4] for converters 5-8

1) dc voltage deviation: As the solid lines in Fig. 14 show, in the proposed scheme, the dc voltages return to the values very close to the level prior to the incidence after some duration. The duration is the time until the converters receive the information about the event from the tripped converter. Table I shows the time delays for each communication link. The dc voltages don't return to the exact pre-disturbance position because of the power losses. As shown in (29), the change in dc voltage magnitude after the activation of the proposed mechanism is influenced by the power loss and the droop constants of converters located in areas #1 and #2. Moreover, comparative analysis is carried out considering the works reported in [23] and [4]. In the case of [23] and [4], the steady-state change of the dc voltage is significant as the dashed and dotted lines in Figs. 14 depict. For instance, the change in the dc voltage of converter #3 is 0.023pu (15kV) in [23] and 0.0342pu (22kV) in [4]. In [23], the dc voltage change is affected by power of the tripped converter before the incidence, the power losses, and the value of the droop constant of the survivor converters of area #3. However, in [4], the dc voltage response is determined by the frequency deviations in addition to the the near mentioned factors for the case of [23] since the technique relies on the conventional frequency droop control.

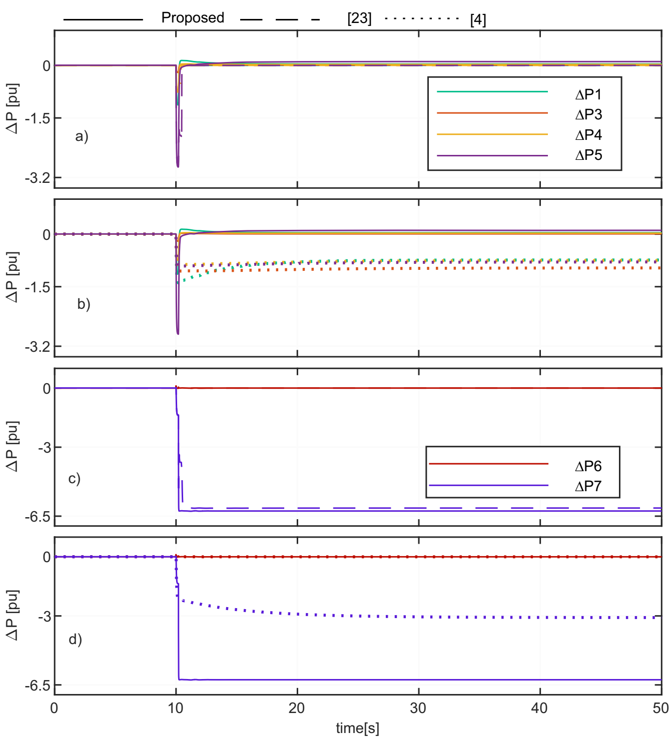

Fig. 15. The loading deviation of survivor converters when converter #6 in area #3 trips a) Proposed vs [23] for converters 1, 3-5 b) Proposed vs [4] for converters 1, 3-5 c) Proposed vs [23] for converters 6-7 d) Proposed vs [4] for converters 6-7

2) frequency deviation: The frequency response of the interconnected areas is shown in Fig. 16. It can be seen that the proposed scheme resulted in very low frequency deviations. Areas #1 and #2 have a frequency deviation of around 0.0315Hz. It was discussed in section V that the power deviation of ac systems without the tripped converter is related to the power losses. The ac power system #3 is expected to have zero frequency deviation since the power transfer with its VSCs is zero. Also, it was shown in the derivation of (30). However, the frequency of area #3 deviates by 0.031Hz as the solid pink line in Fig. 16 illustrates due to the ac power loss. In the case of [23], the change in the frequency of area #1 and #2 is zero since the converters in these areas operate in power control mode keeping their power reference at a value prior to the disturbance. However, the frequency of ac system #3 deviates by around 0.1Hz which is greater than the proposed scheme. On the other hand, looking at the dotted lines in Fig. 16 b), the mechanism in [4] has shown a significant frequency deviation. The magnitude of the deviations are 0.602, 0.514 and 1.38Hz for each area accordingly.

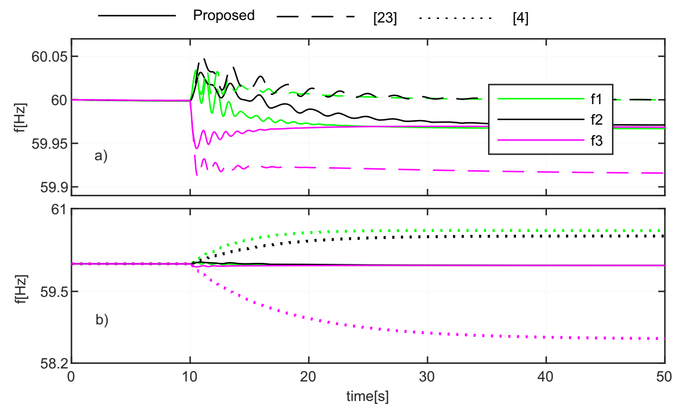

Fig. 16. AC grids frequency response when converter #6 in area #3 trips a) Proposed vs [23] b) Proposed vs [4]

The loading of converters is shown in Fig.15. In the proposed scheme and [23], the survivor converters in area #3 share the burden according to their available headroom. Therefore, converter #8 carry all the power of the tripped converter since converter #7 don't have any more room. In the power response of converter #8, there is a difference between the proposed scheme and [23] as it is described by the solid and the dashed lines in Fig. 15 c). In the proposed scheme, converter #8 operates in power control mode by modifying its power reference according to the pre-incidence loading of converter #6. Hence, the power change of converter #8 is equal to the loading of converter #6 before it trips. On the other hand, in [23], converter #8 works in dc voltage droop control. Therefore, in [23], there will be a mismatch between the pre-incidence power of converter #6 and the change in the power of converter #8 because of the dc network parameters. In [4], the change in the loading of converter #8 is less than the operating power of converter #6 before the incidence. The power responses of converters in area #1 and #2) are presented in Figs.15 a) and b). The converters have small power deviations due to the power losses in the proposed technique and [23]. However, the power deviation is relatively significant in [4] as the dotted lines in Fig.15 b) show.

VIII. Conclusion

An enhanced frequency support strategy is proposed to improve the dc voltage and frequency regulation of high voltage ac/dc power system. Different scenarios such as ac disturbance, converter outage and windfarm power variation are considered in the study. For the case of ac disturbance, the combination of coordinated droop control (CDC) and supplementary controller is developed. In CDC, variable droop gains based on the available capacity of converters are designed to make the ac power systems share the burden according to the specified weights. However, the droop gains can't provide the anticipated performance due to the dc grid and VSCs power losses. Therefore, a supplementary controller is developed so that the interconnected ac areas can share the disturbance according to the desired percentages. Also, the work introduces a novel technique to mitigate the dc voltage and frequency deviation of the ac/dc system during converter outage. Furthermore, the work presents a new droop gain design methodology to distribute the disturbance due to the wind farm power deviation according to the size of the ac power systems.

The proposed mechanism was evaluated for different cases using simulation tests. The augmented controller accurately achieves the specified weights of disturbance sharing among the interconnected asynchronous ac areas during ac disturbance compared to the existing techniques in the literature. In addition, for the conducted test scenario, the maximum frequency deviation is 0.51Hz in the proposed scheme while in CFSS [23] it is 0.83Hz. Also, during converter outage, the presented mechanism almost eliminates the dc voltage and frequency deviation of the ac/dc grid. There is only a small mismatch from zero deviation due to the dc grid and VSCs power losses. However, the dc voltage deviation in the case of CFSS reaches up to 15kV during the considered test case. Furthermore, the ac areas share the stress due to the wind farm power deviation according to their strength. In future, the presented work can be extended to consider the allocation of burden to converters (particularly those located in the same ac grid) during frequency support to be according to their relative distance with respect to the location of the disturbance as this can help to improve the rate of change of frequency (RoCoF). However, for this, the converters need a mechanism to detect how near is the disturbance to them. In our proposed mechanism, converters have the algorithm only to detect the ac area at which the disturbance occurs.

References

[1] P. McNamara and F. Milano, "Model Predictive Control-Based AGC for Multi-Terminal HVDC-Connected AC grids," in IEEE Transactions on Power Systems, vol. 33, no. 1, pp. 1036-1048, Jan. 2018.

[2] J. -S. Kim, J. -Y. Park, Y. -J. Kim and O. Gomis-Bellmunt, "Decentralized Robust Frequency Regulation of Multi-terminal HVDC-linked Grids," in IEEE Transactions on Power Systems, 2022, to be published. doi: 10.1109/TPWRS.2022.3201316.

[3] M. Andreasson, R. Wiget, D. V. Dimarogonas, K. H. Johansson and G. Andersson, " Distributed Frequency Control Through MTDC Transmission Systems," in IEEE Transactions on Power Systems, vol. 32, no. 1, pp. 250-260, Jan. 2017.

[4] N. R. Chaudhuri, R. Majumder and B. Chaudhuri, "System Frequency Support Through Multi-Terminal DC (MTDC) Grids," in IEEE Trans. on Power Syst., vol. 28, no. 1, pp. 347-356, Feb. 2013.

[5] W. Wang, Y. Li, Y. Cao, U. H¨ager and C. Rehtanz, "Adaptive Droop Control of VSC-MTDC System for Frequency Support and Power Sharing," in IEEE Trans. on Power Syst., vol. 33, no. 2, pp. 1264-1274, March 2018.

[6] R. Wang, L. Chen, T. Zheng and S. Mei, "VSG-based adaptive droop control for frequency and active power regulation in the MTDC system," in CSEE Journal of Power and Energy Systems, vol. 3, no. 3, pp. 260-268, Sept. 2017.

[7] Y. Xiong et al., Y. Xiong et al., "Adaptive Dual Droop Control of MTDC Integrated Offshore Wind Farms for Fast Frequency Support," in IEEE Transactions on Power Systems, to be published. doi:doi: 10.1109/TPWRS.2022.3179504.

[8] H. Shadabi and I. Kamwa, "Dual Adaptive Nonlinear Droop Control of VSC-MTDC System for Improved Transient Stability and Provision of Primary Frequency Support," in IEEE Access, vol. 9, pp. 76806-76815, 2021.

[9] Y. Xiong et al., "Improved Communication-Free Coordinated Control of VSC-MTDC Integrated Offshore Wind Farms for Onshore System Frequency Support," in IEEE Transactions on Power Delivery, to be published. doi: 10.1109/TPWRD.2022.3184497.

[10] C. Liu, H. Liu, S. Jiang and L. Zheng, "A novel dynamic additional frequency control strategy for VSC-MTDC system," in CSEE Journal of Power and Energy Systems, to be published. doi: 10.17775/CSEE-JPES.2021.01790.

[11] K. Rouzbehi, W. Zhang, J. Ignacio Candela, A. Luna, and P. Rodriguez, " Unified reference controller for flexible primary control and inertia sharing in multi-terminal voltage source converter-HVDC grids," IET Gener.,Trans. Distrib., vol. 11, no. 3, pp. 750–758, 2017.

[12] Y. Wen, J. Zhan, C. Y. Chung and W. Li, "Frequency Stability Enhancement of Integrated AC/VSC-MTDC Systems With Massive Infeed of Offshore Wind Generation," in IEEE Trans. on Power Syst., vol. 33, no. 5, pp. 5135-5146, Sept. 2018.

[13] Z. Li, Z. Wei, R. Zhan, Y. Li, Y. Tang and X. -P. Zhang, "Frequency Support Control Method for Interconnected Power Systems Using VSCMTDC," in IEEE Trans. on Power Syst., vol. 36, no. 3, pp. 2304-2313, May 2021.

[14] Q. Zhang et al., "Primary Frequency Support Through North American Continental HVDC Interconnections With VSC-MTDC Systems," in IEEE Trans. on Power Syst., vol. 36, no. 1, pp. 806-817, Jan. 2021.

[15] Shinoda, Kosei; Bakhos, Gianni; Gonzalez-Torres, Juan Carlos; Dai, Jing; Benchaib, Abdelkrim "FCR Provisions by Multi-Terminal HVDC System". TechRxiv. Preprint. https://doi.org/10.36227/techrxiv.16644952.v1

[16] A. Kirakosyan, E. F. El-Saadany, M. S. E. Moursi and M. M. A. Salama, "Selective Frequency Support Approach for MTDC Systems Integrating Wind Generation," in IEEE Trans. on Power Syst., vol. 36, no. 1, pp. 366-378, Jan. 2021.

[17] F. D. Bianchi and J. L. Domnguez-Garca, "Coordinated Frequency Control Using MT-HVDC Grids With Wind Power Plants," in IEEE Trans. on Sustain. Energy, vol. 7, no. 1, pp. 213-220, Jan. 2016.

[18] W. Wang, X. Yin, Y. Cao, L. Jiang and Y. Li, "A Distributed Cooperative Control Based on Consensus Protocol for VSC-MTDC Systems," in IEEE Trans. on Power Syst., vol. 36, no. 4, pp. 2877-2890, July 2021.

[19] Y. Li et al, "Novel MTDC droop scheme with decoupled power control for enhancing frequency stabilities of weak AC systems", IET Renew.Power Gener., 2020, Vol. 14 Iss. 11, pp. 2007-2016

[20] S. G. Vennelaganti and N. R. Chaudhuri, "Ratio-Based Selective Inertial and Primary Frequency Support Through MTDC Grids With Offshore Wind Farms," in IEEE Trans. on Power Syst., vol. 33, no. 6, pp. 7277-7287, Nov. 2018.

[21] A. Kirakosyan, E. F. El-Saadany, M. S. E. Moursi and M. M. A. Salama, " An Improved Frequency Support Algorithm for MT-HVDC Systems," in IEEE Transactions on Power Delivery, vol. 37, no. 3, pp. 1916-1929, June 2022.

[22] S. G. Vennelaganti and N. R. Chaudhuri, "Selective Power Routing in MTDC Grids for Inertial and Primary Frequency Support," in IEEE Trans. on Power Syst., vol. 33, no. 6, pp. 7020-7030, Nov. 2018.

[23] B. Ayalew, M. S. E. Moursi and E. F. El-Saadany, " Primary Frequency Support Strategy for MTDC System With Enhanced DC Voltage Response," in IEEE Transactions on Power Systems, vol. 38, no. 2, pp. 1512-1528, March 2023.

[24] H. Dong, Z. Xu, P. Song, G. Tang, Q. Xu and L. Sun, "Optimized Power Redistribution of Offshore Wind Farms Integrated VSC-MTDC Transmissions After Onshore Converter Outage," in IEEE Trans. on Ind. Electron., vol. 64, no. 11, pp. 8948-8958, Nov. 2017.

[25] B. Berggren, K. Lindén and R. Majumder, "DC Grid Control Through the Pilot Voltage Droop Concept—Methodology for Establishing Droop Constants," in IEEE Transactions on Power Systems, vol. 30, no. 5, pp. 2312-2320, Sept. 2015

[26] N. R. Chaudhuri and B. Chaudhuri, "Adaptive Droop Control for Effective Power Sharing in Multi-Terminal DC (MTDC) Grids," in IEEE Transactions on Power Systems, vol. 28, no. 1, pp. 21-29, Feb. 2013.

[27] S. Akkari, M. Petit, J. Dai and X. Guillaud, "Interaction between the Voltage-Droop and the Frequency-Droop Control for Multi-Terminal HVDC Systems," 11th IET International Conference on AC and DC Power Transmission, Birmingham, 2015, pp. 1-7, doi: 10.1049/cp.2015.0036.

[28] S. Akkari, J. Dai, M. Petit, and X. Guillaud, "Interaction between the voltage-droop and the frequency-droop control for multi-terminal HVDC systems," IET Generation, Transmiss. Distrib., vol. 10, no. 6, pp. 1345–1352, 2016

[29] I. M. Sanz, B. Chaudhuri and G. Strbac, "Frequency changes in AC systems connected to DC grids: Impact of AC vs. DC side events," 2014 IEEE PES General Meeting — Conference & Exposition, National Harbor, MD, USA, 2014, pp. 1-5, doi: 10.1109/PESGM.2014.6939914.

[30] P. Kundur, N. J. Balu, and M. G. Lauby, Power System Stability and Control. vol. 7. New York, NY, USA: McGraw-Hill, 1994.

[31] "National Grid powers up world's longest subsea interconnector between the UK and Norway", (accessed on March 1, 2022). [Online]. Available: https://www.nationalgrid.com/national-grid-powers-worlds-longest-subsea-interconnector-between-uk-and-norway.

[32] N. R. Chaudhuri, B. Chaudhuri, R. Majumder, and A. Yazdani, Multi-terminal Direct Current Grids: Modeling, Analysis, and Control. Oxford, U.K.: Wiley, 2014.

[33] B. Ayalew, M. S. E. Moursi and E. F. El-Saadany, " Enhanced DC Voltage Regulation and Transient Response for Multi-Terminal VSC-HVDC System Using Direct Power Control," in IEEE Transactions on Power Systems, vol. 37, no. 4, pp. 2538-2548, July 2022.

[34] J. Beerten, S. Cole and R. Belmans, "Generalized Steady-State VSC MTDC Model for Sequential AC/DC Power Flow Algorithms," in IEEE Trans. on Power Syst., vol. 27, no. 2, pp. 821-829, May 2012.

[35] "Balancing and Frequency Control ," (accessed on July 1, 2022) Available: https://www.nerc.com

Biyadgie Ayalew received the MSc degree in sustainable transportation and electric power system (STEPS), an Erasmus Mundus Program coordinated by the University of Oviedo, in Spain, University of Nottingham, in the UK, and Polytechnique Institute of Coimbra, in Portugal, in 2016, and the PhD degree in electrical engineering from Khalifa University, Abu Dhabi, UAE, in 2022. Currently, he is working as Postdoctoral fellow in Khalifa University, Abu Dhabi, UAE. His current research interests include modeling and control of multi-terminal HVDC system for interconnection of ac grids and integration of wind farms.

Mohamed Shawky El Moursi (M'12, SM15) received the B.Sc. and M.Sc. degrees from Mansoura University, Mansoura, Egypt, in 1997 and 2002, respectively, and the Ph.D. degree from the University of New Brunswick (UNB), Fredericton, NB, Canada, in 2005, all in electrical engineering. He was a Research and Teaching Assistant in the Department of Electrical and Computer Engineering, UNB, from 2002 to 2005. He joined McGill University as a Postdoctoral Fellow with the Power Electronics Group. He worked at Vestas Wind Systems, Arhus, Denmark, in the Technology R&D with the Wind Power Plant Group. He was with TRANSCO, UAE, as a Senior Study and Planning Engineer. He is currently a Professor in the Electrical Engineering and Computer Science Department and the Acting Director of Advanced Power and Energy Center (APEC) at Khalifa University and seconded to a distinguished Professor position in the Faculty of Engineering, Mansoura University, Egypt and currently on leave. He was a Visiting Professor at Massachusetts Institute of Technology, Cambridge, Massachusetts, USA. Dr. Shawky is currently an Editor of IEEE Transactions on Power Delivery, IEEE Transactions on Power Systems, Associate Editor of IEEE Transactions on Power Electronics, Associate Editor of IEEE Transactions on Smart Grid, Guest Editor of IEEE Transactions on Energy Conversion, Guest Editor-in-Chief for special section between TPWRD and TPWRS, Editor for IEEE Power Engineering Letters, Regional Editor for IET Renewable Power Generation and Associate Editor for IET Power Electronics Journals. His research interests include renewable energy systems (Wind and PV) integration, power system, FACTS technologies, VSC-HVDC systems, Microgrid operation and control and AI applications in Power Systems.

Ehab F. El-Saadany (F'18) was born in Cairo, Egypt, in 1964. He received the B.Sc. and M.Sc. degrees in Electrical Engineering from Ain Shams University, Cairo, Egypt, in 1986 and 1990, respectively, and the Ph.D.degree in Electrical Engineering from the University of Waterloo, Waterloo, ON, Canada, in 1998, where he was a Professor with the ECE Department till 2019. Currently he is a Professor in EECS Department and the Director of the Advanced Power and Energy Research Center at Khalifa University, Abu Dhabi, UAE. His research interests include smart grid operation and control, microgrids, self healing, power quality, distributed generation, power electronics interfacing, and mechatronics. He is an Editor of the IEEE TRANSACTIONS ON SMART GRID, IEEE TRANSACTIONS ON POWER SYSTEMS and IEEE Power Systems Letters. He is a Registered Professional Engineer in the Province of Ontario.